Dimanganese(II) Complexes of a New Phenol-based Dinucleating Ligand with Two Amino Chelating Arms: Synthesis, Structure and Catalase-like Activity†

Chikako Higuchi,[a] Hiroshi Sakiyama,*[,a] Hisashi Ōkawa*[,a] and David E. Fenton[b]
[a] *Department of Chemistry, Faculty of Science, Kyushu University, Hakozaki, Higashi-ku, Fukuoka 812, Japan*
[b] *Department of Chemistry, The University of Sheffield, Sheffield S3 7HF, UK*

A new phenol-based dinucleating ligand with two amino chelating arms, 2,6-bis{[*N*-(2-dimethylaminoethyl)-*N*-methyl]aminomethyl}-4-methylphenolate (L^-), formed dinuclear manganese(II) complexes $[Mn_2L(p\text{-}XC_6H_4CO_2)_2(NCS)(MeOH)]$ (X = H **1**, Cl **2**, Me **3** or NO_2 **4**). X-Ray analysis revealed that complex **1** crystallizes in the monoclinic space group $P2_1/c$, a = 12.607(3), b = 19.566(6), c = 16.743(5) Å and β = 107.56(2)°. The two manganese ions are bridged by the phenolic oxygen and two benzoate groups. The NCS^- ion is co-ordinated to one of the manganese ions through its nitrogen and the methanol molecule to the other, providing distorted-octahedral geometries around each manganese. Magnetic susceptibility measurements over the temperature range 4.2–300 K indicated a weak antiferromagnetic interaction (J = −3 to −5 cm^{-1} based on $\hat{H} = -2J\hat{S}_1\cdot\hat{S}_2$). The complexes show a catalase-like activity in disproportionating H_2O_2 in dimethylformamide. The rate of dioxygen evolution was proportional to the concentration of H_2O_2 and the rate constant decreased in the order **1** (X = H) > **2**(Cl) > **3**(Me) > **4**(NO_2).

Manganese catalases are non-haem enzymes which catalyse the disproportionation of hydrogen peroxide into water and molecular oxygen and have been isolated from *Thermus thermophilus*, *Lactobacillus plantarum* and *Thermoleophilum album*.[1] They are known to contain two manganese ions at their active centre[2] and the μ-oxo-bis(μ-carboxylato)dimanganese(III) core has been suggested as a promising candidate for this.[3] It is generally believed that the disproportionation reaction is catalysed by the interconversion of the two oxidation states $Mn^{III}Mn^{III}$ and $Mn^{II}Mn^{II}$.[4] However, the active-site structure is not proven and the H_2O_2 disproportionation mechanism remains unclear.

At this stage a bioinorganic approach using simple model complexes is of value in order to gain insight into the structure and catalytic mechanism of manganese catalase.[3,5] In our recent model studies[6–8] using μ-phenoxo-bis(μ-carboxylato)dimanganese(II) core complexes derived from the phenol-based compound $(L^1)^-$ and $(L^2)^-$, a $\{Mn^{IV}(=O)\}_2$ species has been detected as an active intermediate in the disproportionation of H_2O_2 using mass spectrometry and visible spectroscopy. It is presumed that the step $Mn^{III}Mn^{III} \longrightarrow Mn^{IV}Mn^{IV}$ is involved in the catalytic H_2O_2 disproportionation by these complexes. One noticeable difference in catalytic activity between the complexes of $(L^1)^-$ and those of $(L^2)^-$ is in the total amount of O_2 evolved. This amount was nearly theoretical for the former complexes, but *ca.* 70% for the latter. It should be noted that $(L^1)^-$ is symmetric whereas $(L^2)^-$ is unsymmetric with respect to the articular nitrogens; two imino groups in the former and one amino and one imino group in the latter. It appears that a side reaction occurs to consume H_2O_2 when a pair of manganese ions are not equivalent electronically.[7,8]

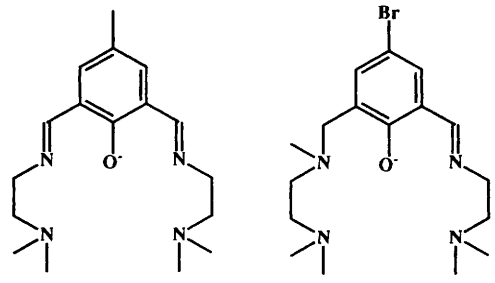

$(L^1)^-$ $(L^2)^-$

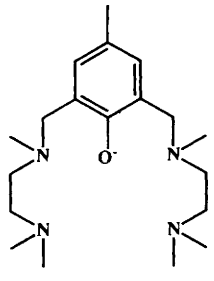

L^-

The present study has been undertaken in order to obtain further support for the significance of the core structure and in the presence of an equivalent pair of manganese ions as regards catalase-like activity. 2,6-Bis{[*N*-(2-dimethylaminoethyl)-*N*-methyl]aminomethyl}-4-methylphenolate (L^-) has been prepared and is symmetric with respect to the two articular amino groups. Dinuclear manganese(II) complexes of general formula $[Mn_2L(p\text{-}XC_6H_4CO_2)_2(NCS)(MeOH)]$ (X = H **1**, Cl **2**, Me **3** or NO_2 **4**) have been obtained and their catalytic activity towards the decomposition of H_2O_2 has been studied.

† *Supplementary data available:* see Instructions for Authors, *J. Chem. Soc., Dalton Trans.*, 1995, Issue 1, pp. xxv–xxx.
Non-SI unit employed: $\mu_B \approx 9.27 \times 10^{-24}$ J T^{-1}.

Experimental

Materials.—All chemicals were of reagent grade and used as purchased.

Measurements.—Elemental analyses of C, H and N were obtained at the Service Centre of Elemental Analysis, Kyushu University. Analyses of manganese were made on a Shimadzu AA-680 atomic absorption/flame emission spectrophotometer. Infrared (IR) spectra were recorded on KBr discs with a JASCO IR-810 spectrophotometer. Molar conductances were measured on a DKK AOL-10 conductivity meter at room temperature. Electronic spectra were recorded on a Shimadzu MPS-2000 spectrophotometer at room temperature, ^{1}H NMR spectra (400 MHz) on a JEOL JNM-GX 400 spectrometer in $CDCl_3$ using tetramethylsilane as internal standard and electron impact (EI) mass spectra on a Hitachi M-60 mass spectrometer. Magnetic susceptibilities were measured on a HOXAN HSM-D SQUID susceptometer in the temperature range 4.2–80 K and a Faraday balance in the range 80–300 K. Calibrations were made with $[NH_4]_2Mn[SO_4]_2{\cdot}6H_2O$ for the SQUID magnetometer and with $[Ni(en)_3][S_2O_3]$ (en = ethane-1,2-diamine) for the Faraday balance.[9] Effective magnetic moments were calculated by the equation $\mu_{eff} = 2.828(\chi_A T)^{\frac{1}{2}}$ where χ_A is the magnetic susceptibility corrected for diamagnetism of the constituting atoms using Pascal's constants.[10] Cyclic voltammograms were recorded in CH_2Cl_2 on a glassy carbon working electrode, using tetra-*n*-butylammonium perchlorate as the supporting electrolyte. **CAUTION**: this perchlorate is explosive and should be handled with great care!

Preparations.—*2,6-Bis*{[*N*-(*2-dimethylaminoethyl*)-*N-methyl*]-*aminomethyl*}-*4-methylphenol trihydrobromide* (HL·3HBr). This was prepared by the modification[11] of a Mannich reaction. 4-Methylphenol (5.5 g, 50 mmol), *N,N,N'*-trimethylethane-1,2-diamine (10.2 g, 100 mmol) and paraformaldehyde (4.0 g, 134 mmol) were refluxed in ethanol (150 cm^3) for 8 h. The resulted yellow solution was cooled to room temperature, acidified with hydrobromic acid (48%, 15 cm^3), and evaporated to dryness to give a pale yellow oil. It was dissolved in ethanol (100 cm^3) and concentrated to a small portion to give a white precipitate. This was filtered off and dried *in vacuo*. Yield: 14.4 g (50%) (Found: C, 39.10; H, 6.85; N, 9.40. Calc. for $C_{19}H_{39}Br_3N_4O$: C, 39.40; H, 6.80; N, 9.65%).

The free compound HL was obtained as a colourless oil by neutralizing the trihydrobromide with $NaHCO_3$. ^{1}H NMR ($CDCl_3$): δ 2.22 (s, 3 H), 2.23 (s, 12 H), 2.27 (s, 6 H), 2.47–2.59 (m, 8 H), 3.58 (s, 4 H) and 6.85 (s, 2 H). Positive EI mass spectrum; *m/z* 336.

$[Mn_2L(PhCO_2)_2(NCS)(MeOH)]$ **1**. A solution of HL·3HBr (0.290 g, 0.5 mmol) and $LiOH{\cdot}H_2O$ (0.063 g, 1.5 mmol) in methanol (10 cm^3) was added to manganese(II) benzoate tetrahydrate (0.369 g, 1.0 mmol) and the mixture stirred for 10 min. Addition of NaSCN (0.081 g, 1.0 mmol) yielded a white precipitate. Yield: 0.321 g (84%) (Found: C, 53.80; H, 6.30; Mn, 14.45; N, 9.00. Calc. for $C_{35}H_{49}Mn_2N_5O_6S$: C, 54.05; H, 6.35; Mn, 14.10; N, 9.00%). Selected IR data ($\tilde{\nu}$/cm^{-1}), KBr disc: 3000–2800 [ν(C–H)], 2080 [ν(C–N) of isothiocyanate], 1610, 1570 [ν_{asym}(C–O) of benzoate], 1475, 1400 [ν_{sym}(C–O) of benzoate], 1310 and 720. Molar conductance (Λ_M/S cm^2 mol^{-1}) in dimethylformamide (dmf): 65. UV/VIS [λ_{max}/nm (ε/dm^3 mol^{-1} cm^{-1})] in dmf: 278 (2300) and 304 (3900).

$[Mn_2L(p\text{-}ClC_6H_4CO_2)_2(NCS)(MeOH)]{\cdot}H_2O$ **2**. This complex was synthesized under an argon atmosphere. A solution of HL·3HBr (0.290 g, 0.5 mmol), $LiOH{\cdot}H_2O$ (0.063 g, 1.5 mmol) and *p*-chlorobenzoic acid (0.310 g, 2.0 mmol) in methanol (10 cm^3) was added to a methanol solution of manganese(II) perchlorate tetrahydrate (0.369 g, 1.0 mmol). Then triethylamine (1 cm^3) was added and the mixture stirred for 10 min. The addition of NaSCN (0.081 g, 1.0 mmol) yielded a white precipitate. Yield: 0.362 g (84%) (Found: C, 48.45; H, 5.35; Mn, 12.60; N, 8.10. Calc. for $C_{35}H_{49}Cl_2Mn_2N_5O_7S$: C, 48.60; H, 5.70; Mn, 12.70, N, 8.10%). Selected IR data ($\tilde{\nu}$/cm^{-1}), KBr disc: 3000–2800 [ν(C–H)], 2060 [ν(C–N) of isothiocyanate], 1615, 1560 [ν_{asym}(C–O) of benzoate], 1480, 1405 [ν_{sym}(C–O) of benzoate], 780 and 540. Molar conductance (Λ_M/S cm^2 mol^{-1}) in dmf: 51. UV/VIS [λ_{max}/nm (ε/dm^3 mol^{-1} cm^{-1})] in dmf: 278 (3300) and 303 (5000).

$[Mn_2L(p\text{-}MeC_6H_4CO_2)_2(NCS)(MeOH)]{\cdot}H_2O$ **3**. This was prepared as a beige powder by a method similar to that for complex **2**, using *p*-methylbenzoic acid instead of *p*-chlorobenzoic acid. Yield: 0.168 g (41%) (Found: C, 54.20; H, 6.30; Mn, 13.10; N, 8.45. Calc. for $C_{37}H_{55}Mn_2N_5O_5S$: C, 53.95; H, 6.35; Mn, 13.30; N, 8.50%). Selected IR data ($\tilde{\nu}$/cm^{-1}), KBr disc: 3000–2800 [ν(C–H)], 2060 [ν(C–N) of isothiocyanate], 1610, 1560 [ν_{asym}(C–O) of benzoate], 1475, 1465, 1400 [ν_{sym}(C–O) of benzoate] and 770. Molar conductance (Λ_M/S cm^2 mol^{-1}) in dmf: 66. UV/VIS [λ_{max}/nm (ε/dm^3 mol^{-1} cm^{-1})] in dmf: 281 (2800) and 303 (4500).

$[Mn_2L(p\text{-}O_2NC_6H_4CO_2)_2(NCS)(MeOH)]$ **4**. This was prepared as a pale yellow powder by a method similar to that for complex **2**, using *p*-nitrobenzoic acid instead of *p*-chlorobenzoic acid in air. Yield: 0.236 g (54%) (Found: C, 48.30; H, 5.20; Mn, 12.70; N, 11.55. Calc. for $C_{35}H_{47}Mn_2N_7O_{10}S$: C, 48.45; H, 5.45; Mn, 12.70; N, 11.30%). Selected IR data ($\tilde{\nu}$/cm^{-1}), KBr disc: 3000–2800 [ν(C–H)], 2060 [ν(C–N) of isothiocyanate], 1630, 1590 [ν_{asym}(C–O) of benzoate], 1520, 1470, 1410 [ν_{sym}(C–O) of benzoate], 1340, 1310, 800 and 720. Molar conductance (Λ_M/S cm^2 mol^{-1}) in dmf: 64. UV/VIS [λ_{max}/nm (ε/dm^3 mol^{-1} cm^{-1})] in dmf: 300 (sh) (23 000).

Single-crystal X-Ray Analysis of Complex **1**.—*Crystal data.* $C_{35}H_{49}Mn_2N_5O_6S$, M = 777.74, monoclinic, space group $P2_1/c$, a = 12.607(3), b = 19.566(6), c = 16.743(5) Å, β = 107.56(2)°, U = 3937(2) Å^3, D_c = 1.312 g cm^{-3}, Z = 4, F(000) = 2535, μ(Mo-Kα) = 7.12 cm^{-1}.

Data collection and reduction. Single crystals of complex **1** were obtained by slow recrystallization from methanol. One with approximate dimensions 0.5 × 0.4 × 0.4 mm was used. Intensities and lattice parameters were obtained on a Rigaku AFC-5 automated four-circle diffractometer, with graphite-monochromated Mo-Kα radiation (λ = 0.710 69 Å) at 20 ± 1 °C. Lattice parameters and their estimated standard deviations were obtained from a least-squares fit to 25 reflections in the range 25 < 2θ < 30°. For the intensity-data collections the ω–2θ scan mode was used at a scan rate of 2° min^{-1}. The octant measured was ±h, +k, +l. Three standard reflections were monitored every 100 and showed no systematic decrease in intensity. The intensity data were corrected for Lorentz and polarization factors. 2535 Independent reflections with $F > 3\sigma(F)$ in the range 2.5 ≤ 2θ ≤ 45° were used for the analysis.

The structure was solved by the heavy-atom method. Refinement was carried out by block-diagonal least squares, the function minimized being $\Sigma w(|F_o| - |F_c|)^2$ with weights w = 1. Atomic scattering factors were taken from ref. 12. Hydrogen atoms were fixed at the calculated positions and were not refined. The final values of R and R' were 0.0973 and 0.1043, respectively ($R = \Sigma||F_o| - |F_c||/\Sigma|F_o|$, $R' = \{\Sigma[w(|F_o| - |F_c|)^2]/\Sigma[w|F_o|^2]\}^{\frac{1}{2}}$. All calculations were carried out on a FACOM M-1800/20 computer in the Computer Centre of Kyushu University by use of a local version[13] of the UNICS III[14] and ORTEP[15] programs.

The final positional parameters of non-hydrogen atoms with their estimated standard deviations are listed in Table 1.

Additional material available from the Cambridge Crystallographic Data Centre comprises H-atom coordinates, thermal parameters and remaining bond lengths and angles.

Results and Discussion

Crystal Structure of Complex **1**.—The structure of complex **1** is shown in Fig. 1; selected bond distances and bond angles are

Table 1 Atomic coordinates ($\times 10^4$) for non-hydrogen atoms in complex **1**

Atom	x	y	z	Atom	x	y	z
Mn(1)	7 972(2)	2 675(1)	3 499(1)	C(19)	5 392(18)	5 092(13)	1 163(15)
Mn(2)	7 557(2)	4 207(1)	2 254(2)	O(A1)	9 361(9)	2 759(6)	3 052(7)
O(1)	7 650(8)	3 742(5)	3 456(6)	O(A2)	9 135(9)	3 756(6)	2 374(8)
N(1)	6 789(10)	2 575(7)	4 337(8)	C(A1)	9 670(12)	3 219(9)	2 662(9)
N(2)	9 233(11)	2 491(8)	4 859(8)	C(A2)	10 840(11)	3 165(7)	2 566(9)
N(3)	8 415(12)	5 163(7)	3 066(9)	C(A3)	11 201(14)	3 656(9)	2 106(11)
N(4)	6 068(11)	5 028(8)	2 061(10)	C(A4)	12 261(15)	3 604(10)	1 999(12)
C(1)	6 864(18)	5 296(11)	6 095(13)	C(A5)	12 916(14)	3 071(11)	2 362(11)
C(2)	7 082(14)	4 871(9)	5 410(11)	C(A6)	12 576(14)	2 578(11)	2 787(13)
C(3)	6 535(13)	4 260(10)	5 134(11)	C(A7)	11 500(14)	2 622(10)	2 901(11)
C(4)	6 713(13)	3 871(10)	4 482(10)	O(B1)	6 653(9)	2 529(6)	2 372(7)
C(5)	7 480(12)	4 105(8)	4 094(10)	O(B2)	6 274(9)	3 519(6)	1 661(7)
C(6)	8 072(13)	4 700(9)	4 401(10)	C(B1)	6 063(11)	2 909(9)	1 790(9)
C(7)	7 863(14)	5 079(9)	5 044(10)	C(B2)	5 022(12)	2 603(9)	1 227(9)
C(8)	6 070(13)	3 204(10)	4 200(11)	C(B3)	4 273(14)	3 010(11)	647(11)
C(9)	6 072(15)	1 989(10)	4 050(14)	C(B4)	3 309(15)	2 726(11)	106(12)
C(10)	7 489(16)	2 515(10)	5 242(11)	C(B5)	3 128(16)	2 045(12)	125(12)
C(11)	8 524(19)	2 170(12)	5 329(12)	C(B6)	3 905(15)	1 626(12)	685(12)
C(12)	10 077(16)	2 000(11)	4 858(14)	C(B7)	4 839(13)	1 891(10)	1 246(10)
C(13)	9 759(20)	3 122(13)	5 213(14)	S	7 934(11)	4 876(6)	−550(7)
C(14)	8 914(13)	4 954(9)	3 967(10)	N(5)	7 679(13)	4 588(9)	1 045(10)
C(15)	9 273(15)	5 399(10)	2 724(13)	C(20)	7 782(19)	4 747(15)	443(15)
C(16)	7 602(16)	5 718(9)	3 005(12)	O(M)	8 089(10)	1 506(6)	3 337(8)
C(17)	6 642(20)	5 689(12)	2 257(17)	C(M)	8 206(23)	1 225(12)	2 585(17)
C(18)	5 353(18)	4 915(15)	2 551(17)				

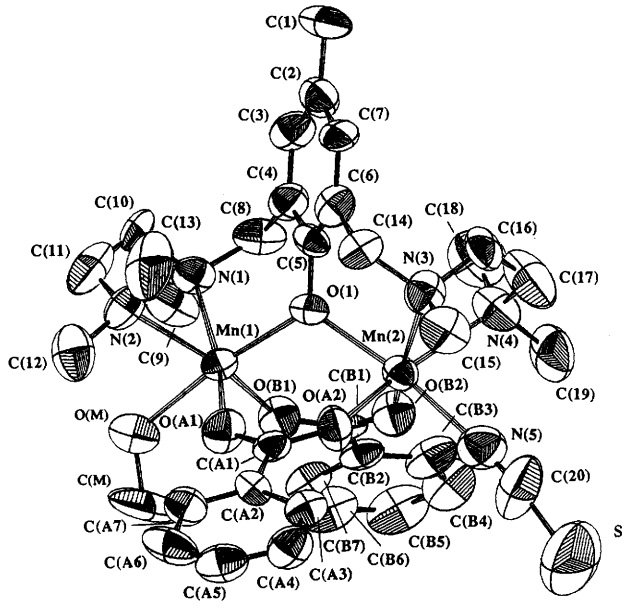

Fig. 1 An ORTEP view of complex **1** with the atom numbering scheme

Table 2 Selected bond distances (Å) and angles (°) for complex **1**

Mn(1)–O(1)	2.124(11)	Mn(1)–N(1)	2.343(16)
Mn(1)–N(2)	2.378(12)	Mn(1)–O(A1)	2.109(13)
Mn(1)–O(B1)	2.125(10)	Mn(1)–O(M)	2.313(13)
Mn(2)–O(1)	2.179(11)	Mn(2)–N(3)	2.373(14)
Mn(2)–N(4)	2.417(15)	Mn(2)–O(A2)	2.131(12)
Mn(2)–O(B2)	2.108(11)	Mn(2)–N(5)	2.207(18)
Mn(1)···Mn(2)	3.598(4)		
O(1)–Mn(1)–N(1)	87.3(5)	O(1)–Mn(1)–N(2)	104.3(5)
O(1)–Mn(1)–O(A1)	94.7(5)	O(1)–Mn(1)–O(B1)	90.7(4)
O(1)–Mn(1)–O(M)	170.5(4)	N(1)–Mn(1)–N(2)	77.1(5)
N(1)–Mn(1)–O(A1)	165.0(4)	N(1)–Mn(1)–O(B1)	93.0(5)
N(1)–Mn(1)–O(M)	93.6(5)	N(2)–Mn(1)–O(A1)	88.0(5)
N(2)–Mn(1)–O(B1)	161.4(5)	N(2)–Mn(1)–O(M)	85.1(4)
O(A1)–Mn(1)–O(B1)	101.9(5)	O(A1)–Mn(1)–O(M)	86.9(5)
O(B1)–Mn(1)–O(M)	79.8(4)	O(1)–Mn(2)–N(3)	85.0(5)
O(1)–Mn(2)–N(4)	103.0(5)	O(1)–Mn(2)–O(A2)	87.2(5)
O(1)–Mn(2)–O(B2)	89.4(4)	O(1)–Mn(2)–N(5)	171.6(5)
N(3)–Mn(2)–N(4)	75.8(5)	N(3)–Mn(2)–O(A2)	91.2(5)
N(3)–Mn(2)–O(B2)	157.8(5)	N(3)–Mn(2)–N(5)	96.5(6)
N(4)–Mn(2)–O(A2)	162.5(5)	N(4)–Mn(2)–O(B2)	84.7(5)
N(4)–Mn(2)–N(5)	85.3(6)	O(A2)–Mn(2)–O(B2)	110.0(5)
O(A2)–Mn(2)–N(5)	84.5(6)	O(B2)–Mn(2)–N(5)	92.3(6)

listed in Table 2. The molecule consists of one ligand L^-, two manganese ions, two benzoate groups, one isothiocyanate ion and one methanol molecule. The two manganese ions are bridged by the phenolic oxygen and two benzoate groups, forming a μ-phenoxo-bis(μ-benzoato)dimanganese(II) core structure. Atom Mn(1) is six-co-ordinated to O(1), N(1) and N(2) of L^-, O(A1) and O(B1) of two benzoate groups and O(M) of the methanol molecule; Mn(2) is also six-co-ordinated with an isothiocyanate nitrogen N(5) as the sixth donor atom. In the related complexes $[Mn_2L^1(PhCO_2)_2(NCS)]$ and $[Mn_2L^2(PhCO_2)_2(NCS)]$ one of the manganese ions is six-co-ordinate with an isothiocyanate nitrogen whereas the other is five-co-ordinate.[6,8,16] It appears that L^- is more flexible for co-ordination, relative to $(L^1)^-$ and $(L^2)^-$, and allows a six-co-ordinate geometry for both manganese ions. The plane defined by Mn(1), Mn(2) and O(1) and the least-squares plane of the aromatic ring of L^- are twisted with a dihedral angle of 55°. The Mn(1)···Mn(2) separation is 3.598(4) Å which is significantly longer than those of related μ-phenoxo-bis(μ-carboxylato)dimanganese(II) complexes (3.2–3.4 Å).[6,8,16,17]

Physicochemical Properties.—Complexes **1**–**4** are stable in the solid state but are gradually oxidized in dmf, changing from yellow to brown. In their IR spectra the symmetric and antisymmetric vibrations, $\nu_{asym}(CO_2)$ and $\nu_{sym}(CO_2)$, of the benzoate group are observed at 1560–1590 and 1400–1410 cm^{-1}, respectively. The small separation between the vibrations (< 200 cm^{-1}) is typical of bridging carboxylate groups,[18] the presence of which is demonstrated above for **1** by X-ray crystallography. The ν(CN) mode of the isothiocyanate group appears at 2060–2080 cm^{-1}, but the ν(CS) and δ(NCS) modes are not resolved.

Table 3 Magnetic data for complexes **1**–**4**[a]

Complex	μ_{eff}/μ_B[b]	J/cm^{-1}	g
1	5.56	−2.9	1.96
2	5.66	−3.2	2.00
3	5.66	−4.5	2.00
4	5.51	−4.1	2.00

[a] N_α fixed at 0 $cm^3\ mol^{-1}$. [b] At room temperature.

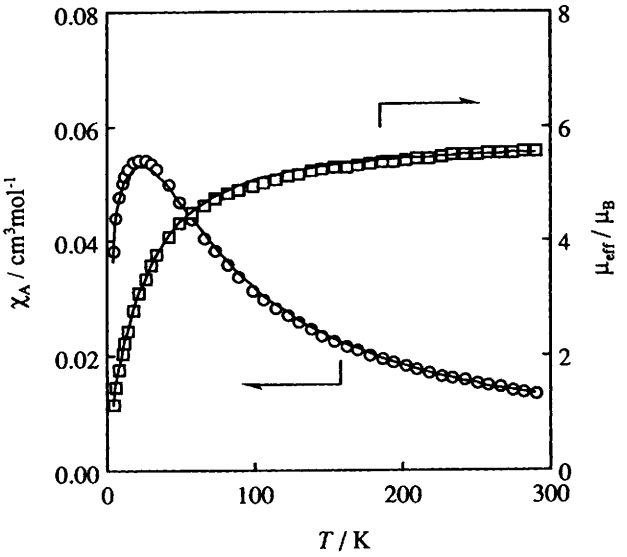

Fig. 2 Temperature dependences of χ_A(○) and μ_{eff}(□) of complex **1**. Solid curves are based on equation (1) in the text, using $J = -2.9\ cm^{-1}$, $g = 1.96$ and $N_\alpha = 0\ cm^3\ mol^{-1}$

The molar conductances of complexes **1**–**4**, at a concentration of 1×10^{-3} mol dm^{-3} in dmf, fall in the range 51–66 S cm^2 mol^{-1} which is typical of 1:1 electrolytes in this solvent.[19] All the complexes show no absorption bands in the region 400–700 nm, suggesting that the manganese(II) ions are in a high-spin state. The strong absorptions near 280 and 300 nm for **1**–**3** are attributed to intraligand transitions. The UV spectrum of **4** differs from those of **1**–**3**, probably because of the superposition of transitions from the *p*-nitrobenzoate group. A cyclic voltammogram of **1** showed two ill defined quasi-reversible couples around 0.55 and 1.00 V *vs.* the saturated calomel electrode. Similarly, for **4** at around 0.75 and 1.00 V. The first couple may be assigned to oxidation of the dimanganese centre and the second to that of the dinucleating ligand.

Magnetic susceptibility measurements for complexes **1**–**4** were made on solid samples in the temperature range 4.2–300 K. The effective magnetic moments at room temperature are in the range 5.51–5.66 μ_B (Table 3), slightly lower than the spin-only value of high-spin Mn^{II}. The magnetic moments decrease with decreasing temperature, suggesting an antiferromagnetic interaction within a pair of manganese(II) ions. The temperature dependences of magnetic susceptibility (χ_A) and effective magnetic moment (μ_{eff}) per Mn for **1** are shown in Fig. 2. The magnetic susceptibility equation for a dinuclear manganese(II) system based on the isotropic Heisenberg model $\hat{H} = -2J\hat{S}_1\cdot\hat{S}_2$ ($S_1 = S_2 = \frac{5}{2}$) is given by equation (1), where

$$\chi_A = \frac{Ng^2\beta^2}{kT}\cdot\frac{x^{28} + 5x^{24} + 14x^{18} + 30x^{10} + 55}{x^{30} + 3x^{28} + 5x^{24} + 7x^{18} + 9x^{10} + 11} + N_\alpha \quad (1)$$

$x = \exp(-J/kT)$, N is the Avogadro number, g the Zeeman splitting factor, β the Bohr magneton, J the exchange integral, k the Boltzmann constant, T the absolute temperature and N_α the temperature-independent paramagnetism. The cryomagnetic property of **1** is well simulated by equation (1), using the parameters $g = 1.96$ and $J = -2.9\ cm^{-1}$ (N_α being assumed to be zero). The reliability factor is defined as $R(\mu) = [\Sigma(\mu_{obs} - \mu_{calc})^2/\Sigma(\mu_{obs})^2]^{\frac{1}{2}}$ is 7.3×10^{-3}. Similarly, the cryomagnetic properties of **2**–**4** are also well reproduced by equation (1). The best-fitting magnetic parameters are given in Table 3. The J values are negative in sign and comparable to those of other μ-phenoxo-bis(μ-carboxylato)dimanganese(II) complexes.[6,8,16,17]

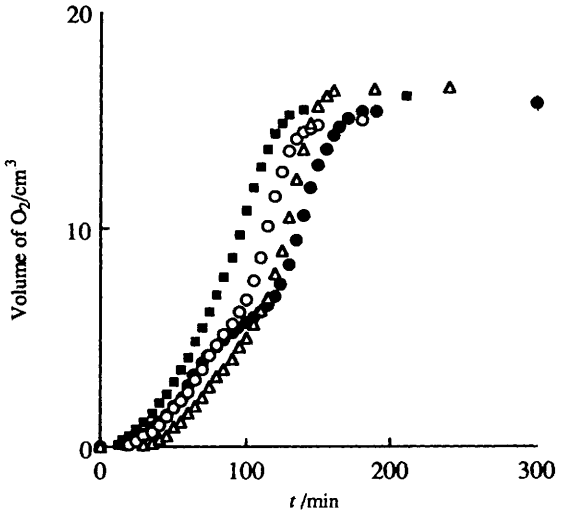

Fig. 3 Time courses for dioxygen evolution in H_2O_2 disproportionation by complexes **1** (△), **2** (○), **3** (■) and **4** (●). Conditions: complex (5 mmol) in dmf (2 cm^3), H_2O_2 (10%, 0.5 cm^3; 1.5 mmol), at 0 °C

Reaction with Hydrogen Peroxide.—The reactivity of complexes **1**–**4** with H_2O_2 was examined in dmf solution at 0 °C. An aqueous H_2O_2 solution was added to a dmf solution of a complex and the volume of O_2 evolved measured using a burette. The total amount of O_2 evolved corresponded to half the equivalent of H_2O_2 added for all the complexes, indicating that all the H_2O_2 disproportionated into O_2 and H_2O [equation (2)]. The time courses of dioxygen evolution are

$$2H_2O_2 \longrightarrow O_2 + 2H_2O \quad (2)$$

shown in Fig. 3. The rate (slope of curve) increased gradually to a maximum and then decreased until all of the H_2O_2 was consumed. At first the reaction mixture was colourless, but then became pink while O_2 was evolved vigorously. When evolution had ceased the pink colour disappeared. The addition of a second portion of H_2O_2 again resulted in the pink colouration and concomitant evolution of O_2. The pink solution showed an absorption band centred around 530 nm on which fine structures, separated by *ca.* 730 cm^{-1}, were imposed (see Fig. 4). The fine structure may be assigned to the ν(Mn=O) vibration coupled to a ligand-to-metal charge-transfer (l.m.c.t.) band from O^{2-} to Mn^{IV} through vibronic interaction.[7,8] This suggests that the $Mn^{IV}(=O)$ species is involved as an active species in the H_2O_2 disproportionation by **1**. No prominent EPR signal was observed for the pink solution in measurements at liquid-nitrogen temperature.

Kinetic studies have been made for the catalase-like reactions of complexes **1**–**4** based on the time courses for dioxygen evolution. Since all the H_2O_2 is disproportionated, the concentration of H_2O_2 at time t, $[H_2O_2]_t$, is estimated by equation (3), where $[H_2O_2]_{init}$ is the initial concentration

$$[H_2O_2]_t = [H_2O_2]_{init} - 2[O_2]_t \quad (3)$$

of H_2O_2 and $[O_2]_t$ is the amount of evolved O_2 (mol dm^{-3}) at time t. It is assumed that the increase in the rate of evolution

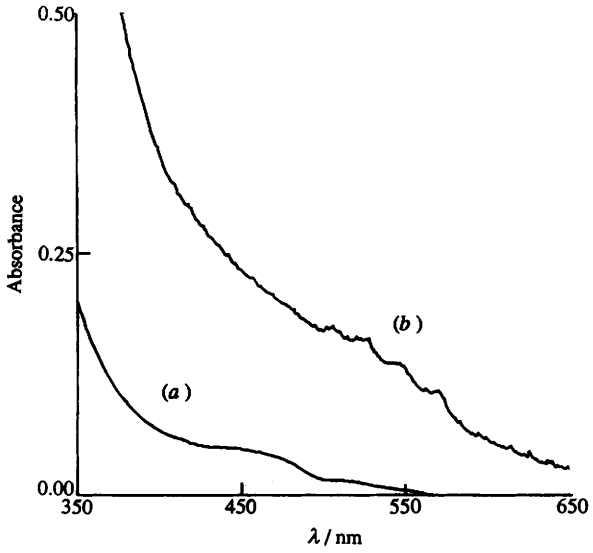

Fig. 4 Visible spectral changes on adding H_2O_2 (9.5%, 0.5 cm^3; 1.40 mmol) to a dmf solution of complex **1** (10^{-3} mol dm^{-3}, 2 cm^3) at 0 °C: (*a*) just after the addition of H_2O_2, (*b*) after 60 min

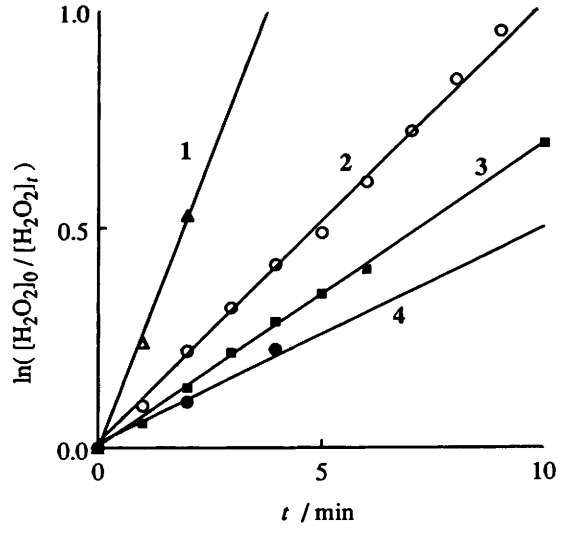

Fig. 5 Plots of $\ln([H_2O_2]_0/[H_2O_2]_t)$ *versus* t for complex **1** (△), **2** (○), **3** (■) and **4** (●)

Table 4 Apparent rate constants for disproportionation of H_2O_2 by complexes **1–4**

Complex	k'/min^{-1}
1	0.26
2	0.10
3	0.069
4	0.049

corresponds to the increase in the active species in solution. Assuming that the concentration of the active species is constant after the evolution rate reaches its maximum, the pseudo-first-order rate equation (4) can be adopted where $[H_2O_2]_0$ is

$$-d[H_2O_2]_t/dt = k'[H_2O_2]_t \quad (4)$$

$$\ln([H_2O_2]_0/[H_2O_2]_t) = k't \quad (5)$$

the concentration of H_2O_2 at the time when the evolution rate reaches the maximum. Plots of $\ln([H_2O_2]_0/[H_2O_2]_t)$ against t [equation (5)] are shown in Fig. 5. Good linearity is obtained for each complex which means that the disproportionation of H_2O_2 is first order in the concentration of H_2O_2 after the

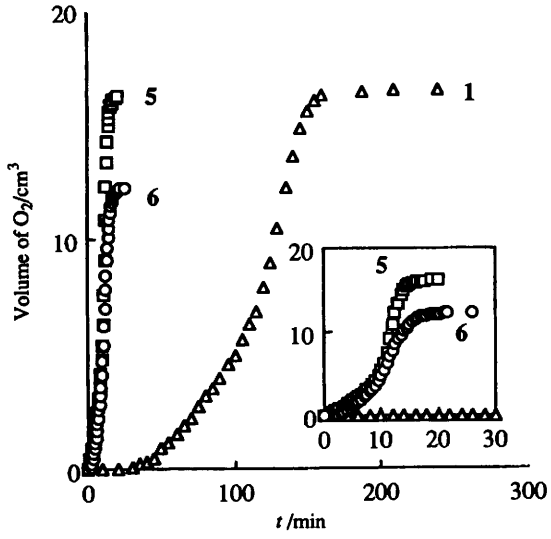

Fig. 6 Time courses of dioxygen evolution in the H_2O_2 disproportionation by complexes **1** (△), **5** (□) and **6** (○). Conditions as in Fig. 3

formation of the active species. The apparent rate constants, k', are summarized in Table 4.

The rate constants decrease in the order **1** (X = H) > **2** (Cl) > **3** (Me) > **4** (NO_2), in accord with increasing bulkiness of the *para*-substituent of the bridging benzoate group. The catalytic activity of the active species should be explained by the electronic effect, but the rate constants are also affected by the concentration of the active species formed in solution. The concentration of the active species is also influenced by both electronic and steric effects. In this case the structural factor seems to be much more important than the electrochemical one.

It is instructive to compare the catalase-like activity of $[Mn_2L(PhCO_2)_2(NCS)(MeOH)]$ **1** with that for $[Mn_2L^1(PhCO_2)_2(NCS)]$[6,7] **5** and $[Mn_2L^2(PhCO_2)_2(NCS)]$[8] **6**. The time courses for dioxygen evolution for the three complexes are shown in Fig. 6 for comparison. As we have reported previously,[8] two different processes are involved in the H_2O_2 disproportionation by **5** and **6**, *i.e.* a slow step A appearing soon after the addition of H_2O_2 and a faster step B appearing after an induction period. In the catalytic disproportionation by **1** the slow process A was not observed and only B was observed after a longer induction period.

We have already shown[6–8] that both complexes **5** and **6** exist as $[Mn_2L^n(PhCO_2)_2]^+$ (n = 1 or 2) in dmf, maintaining the μ-phenoxo-bis(μ-carboxylato)dimanganese(II) core structure. The core structure in dmf solution has approximate C_s symmetry with two vacant or substitution-labile sites in *cis* position, which allows a chelating interaction of H_2O_2 to provide *cis*-$\{Mn^{III}(OH)\}_2$ and then *cis*-$\{Mn^{IV}(=O)\}_2$ species. The intercon-

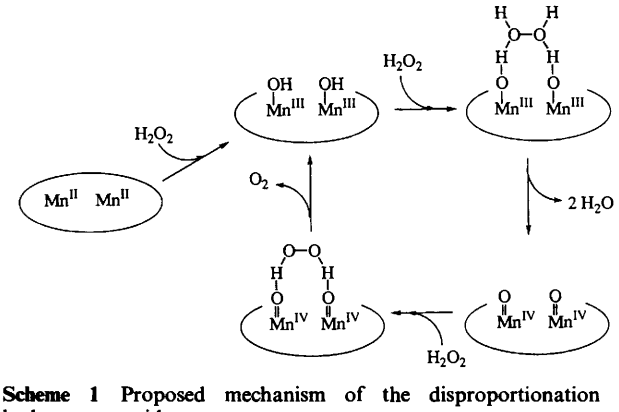

Scheme 1 Proposed mechanism of the disproportionation of hydrogen peroxide

version between the two species through prototropy is essential in the catalytic disproportionation of H_2O_2 by two-electron transfer (Scheme 1). In the case of **1** the isothiocyanate group and methanol molecule may be labile in solution and these two sites are available for H_2O_2 incorporation. Based on the crystal structure of **1**, however, the two donor groups are not situated *cis* but oriented in different directions from each other. In this case the chelating interaction of H_2O_2 with a pair of manganese(II) ions is impossible as long as the core structure is maintained. A possible mechanism is therefore the Haber–Weiss scheme[20] or an intermolecular one. Our recent study has revealed that decomposition of H_2O_2 by an intermolecular mechanism is accompanied more or less by a one-electron reaction, resulting in a reduction of the O_2 evolved.[8,21,22] The quantitative evolution of O_2 in the catalytic decomposition of H_2O_2 by **1–4** thereby suggests an intramolecular two-electron transfer mechanism as proposed for the reaction with **5**.

Thus, it is likely that the dinuclear core of complexes **1–4** can be deformed so as to provide the two labile sites at *cis*-positions for incorporating H_2O_2, to form first *cis*-$\{Mn^{III}(OH)\}_2$ and then *cis*-$\{Mn^{IV}(=O)\}_2$. The involvement of the *cis*-$\{Mn^{IV}(=O)\}_2$ species is supported by the observation of the l.m.c.t. band characteristic of $Mn^{IV}(=O)$. The long induction period in the catalysis by **1–4**, relative to that in the catalysis by **5** and **6**, is explained by the deformation of the initial core structure to form the active intermediates *cis*-$\{Mn^{III}(OH)\}_2$ and *cis*-$\{Mn^{IV}(=O)\}_2$.

In conclusion the catalytic disproportionation of H_2O_2 by complexes **1–4** may proceed by an intramolecular two-electron transfer mechanism through *cis*-$\{Mn^{III}(OH)\}_2$ and *cis*-$\{Mn^{IV}(=O)\}_2$. The yield of O_2 evolved is nearly quantitative in the catalysis by the complexes of the symmetric ligands L^- and $(L^1)^-$; it is less than the theoretical amount in the catalysis by the complexes of the unsymmetric ligand $(L^2)^-$. Thus the present study adds support to the significance of the presence of an equivalent pair of manganese ions in manganese catalase-like activity.

Acknowledgements

We thank Miss Mie Tomono for measurements of ^1H NMR and EI mass spectra and Mr. Masaaki Ohba for help in magnetic measurements. This work was supported by a Grant-in-Aid for Encouragement of Young Scientists (No. 06740511) and by an International Program (No. 06044167) from The Ministry of Education, Science and Culture, Japan.

References

1 R. M. Fronko, J. E. Penner-Hahn and C. J. Bender, *J. Am. Chem. Soc.*, 1988, **110**, 7554; G. S. Allgood and J. J. Perry, *J. Bacteriol.*, 1986, **168**, 563; S. V. Khangulov, V. V. Barynin, V. R. Melik-Adamyan, A. I. Grebenko, N. V. Voyevedskaya, L. A. Blumenfeld, S. N. Dobryakov and V. B. Ilyasova, *Bioorg. Khim.*, 1986, **12**, 741.
2 V. V. Barynin, A. A. Vagin, V. R. Melik-Adamyan, A. I. Grebenko, S. V. Khangulov, A. N. Popov, M. E. Andrianova and B. K. Vainshtein, *Sov. Phys.-Dokl.*, 1986, **31**, 457; Y. Kono and I. Fridovich, *J. Biol. Chem.*, 1983, **258**, 13646; W. F. Beyer, jun., and I. Fridovich, *Biochemistry*, 1985, **24**, 6460.
3 K. Wieghardt, *Angew. Chem., Int. Ed. Engl.*, 1989, **28**, 1153 and refs. therein.
4 G. S. Waldo and J. E. Penner-Hahn, *Biochemistry*, 1995, **34**, 1507; P. J. Pessiki, S. V. Khangulov, D. M. Ho and G. C. Dismukes, *J. Am. Chem. Soc.*, 1994, **116**, 891; P. J. Pessiki and G. C. Dismukes, *J. Am. Chem. Soc.*, 1994, **116**, 898.
5 V. L. Pecoraro, M. J. Baldwin and A. Gelasco, *Chem. Rev.*, 1994, **94**, 807.
6 H. Sakiyama, H. Tamaki, M. Kodera, N. Matsumoto and H. Ōkawa, *J. Chem. Soc., Dalton Trans.*, 1993, 591.
7 H. Sakiyama, H. Ōkawa and R. Isobe, *J. Chem. Soc., Chem. Commun.*, 1993, 882.
8 C. Higuchi, H. Sakiyama, H. Ōkawa, R. Isobe and D. E. Fenton, *J. Chem. Soc., Dalton Trans.*, 1994, 1097.
9 L. F. Lindoy, V. Katovic and D. H. Busch, *J. Chem. Educ.*, 1972, **49**, 117.
10 E. A. Boudreaux and L. N. Mulay, *Theory and Applications of Molecular Paramagnetism*, Wiley, New York, 1976, p. 491.
11 J. D. Crane, D. E. Fenton, J. M. Latour and A. J. Smith, *J. Chem. Soc., Dalton Trans.*, 1991, 2979.
12 *International Tables for X-Ray Crystallography*, Kynoch Press, Birmingham, 1974, vol. 4.
13 S. Kawano, *Rep. Comput. Cent., Kyushu Univ.*, 1983, **16**, 113.
14 T. Sakurai and K. Kobayashi, *Rep. Inst. Phys. Chem. Res.*, 1979, **55**, 69.
15 C. K. Johnson, Report No. ORNL 3794, Oak Ridge National Laboratory, Oak Ridge, TN, 1965.
16 M. Mikuriya, T. Fujii, S. Kamisawa, Y. Kawasaki, T. Tokii and H. Oshio, *Chem. Lett.*, 1990, 1181.
17 M. Suzuki, M. Mikuriya, S. Murata, A. Uehara, H. Oshio, S. Kida and K. Saito, *Bull. Chem. Soc. Jpn.*, 1987, **60**, 4305.
18 G. B. Deacon and R. J. Phillips, *Coord. Chem. Rev.*, 1980, **32**, 227.
19 W. J. Geary, *Coord. Chem. Rev.*, 1971, **7**, 81.
20 F. Haber and J. J. Weiss, *Proc. R. Soc. London, Ser. A*, 1934, **147**, 332.
21 H. Ōkawa and H. Sakiyama, *Pure Appl. Chem.*, 1995, **67**, 273.
22 H. Wada, K. Motoda, M. Ohba, H. Sakiyama, N. Matsumoto and H. Ōkawa, *Bull. Chem. Soc. Jpn.*, 1995, **68**, 1105.

Received 6th July 1995; *Paper* 5/04417K